CHARACTERS OF MARINE ATMOSPHERIC BOUNDARY LAYER STRUCTURE AND AEROSOL PROFILES OBSERVED BY HSRL

Liu Zhi-shen, Yan Zhao-ai, Li Zhi-gang, Guo Jin-jia, Sun Zhao-bin

Ocean Remote Sensing key Laboratory of Ministry of Education,

Ocean University of China, Qingdao, China. Email: lizg@orsi.ouc.edu.cn

ABSTRACT

This paper briefly discusses the aerosol profiles in the marine atmospheric boundary layer (MABL) detected by a high spectral resolution lidar (HSRL) system developed by the Ocean Remote Sensing key Laboratory of the Ministry of Education of China, Ocean University of China (OUC). In this system, iodine filter was used to reject the Mie scattering signal. We got the aerosol scattering ratio (R_b) using the HSRL and analyzed the correlation index of R_b and the Relative Humidity(RH) under different weather conditions, and the height of MABL was derived from the R_b profiles using wavelet method.

1. INTRODUCTION

Atmospheric aerosol varies with time, location and altitude. The component of aerosol are very complicated, which make it difficult to measure its refractive index and extinction property. Few data are available about the aerosol characteristics over the Eastern China Sea.

Lidar provides effective ways of aerosol measurement, She *et al* proposed to measure the vertical profiles of aerosol and atmospheric properties using the high spectral resolution Rayleigh-Mie lidar. *Fischer* used two Fabry-Perot interferometers to detect the vertical profiles of wind and aerosol[1]. We can get the Rayleigh scattering component of atmospheric molecules directly using iodine filter, where iodine filter was used extract the contribution of Rayleigh component by blocking the scattering component of aerosol. Then the scattering ratio measured by lidar was used to calculate aerosol contribution. This kind of high spectral resolution method has potential application in the detection of aerosol in both troposphere and stratosphere, where aerosol are rare. We have built such a high spectral resolution lidar (HSRL) and detected atmospheric aerosol profile successfully.

2. LIDAR SYSTEM AND DATA PROCESSING

The backscattering signals measured by lidar are composed of the contributions from both aerosol and molecules. To detect aerosol, it is necessary to separate the aerosol scattering and molecular scattering. The high spectral resolution lidar (HSRL) with iodine filters has been described by Liu[2] (Fig.1). The master of the system is the two-wavelength diode pumped cw single-mode tunable Nd: YAG seed laser. The

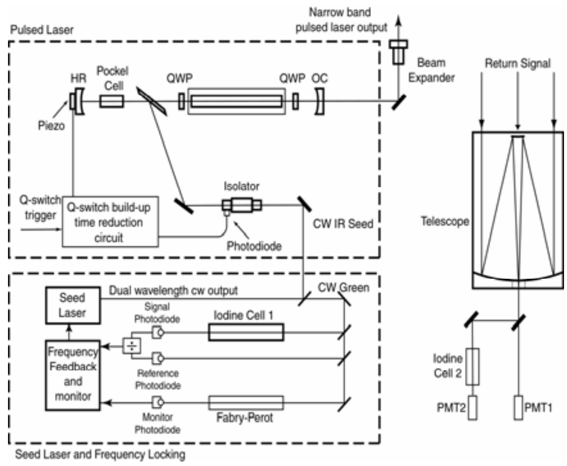

Fig.1. Optical Diagram of HSRL

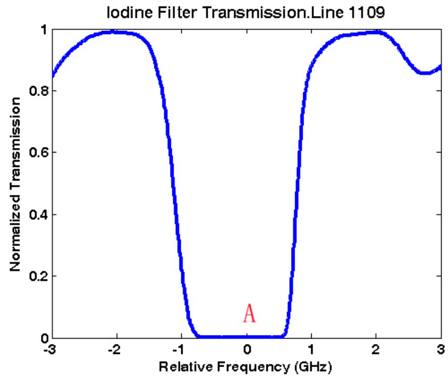

Fig.2. The iodine transmission line of NO.1109 and the lock point A

fundamental output at 1064 nm is used to seed a Continuum Powerlite 7000 Nd: YAG pulsed laser. The 532nm output of the seed laser is sent to iodine filter cell 1 to control and lock the seed laser frequency. Absorption line No.1109 of the iodine is selected for our lidar system. Under the operating conditions, its normalized transmission function is shown in Fig.2. We can measure the aerosol backscattering ratio, $R_b = \beta_\alpha / \beta_m$, using the system by locking the frequency of the seed laser at the 1109 line center of iodine where the aerosol backscattering will be absorbed. The reference channel and the measurement channel are given in Eq.1 and Eq.2 below:

$$N_R = k_R\left(\frac{\Delta r}{r^2}\right)[\beta_a+\beta_m]\exp\left(-2\int dr[\alpha_a(r')+\alpha_m(r')]\right) \qquad (1)$$

$$N_M = k_M\left(\frac{\Delta r}{r^2}\right)[f_a\beta_a+f_m\beta_m]\exp\left(-2\int dr[\alpha_a(r')+\alpha_m(r')]\right) \qquad (2)$$

Where:

$$f_a(\nu) = F(\nu) \quad (3)$$

$$f_m(T,P,\nu) = \int \Re(\nu' - \nu, T, P) F(\nu') d\nu' \quad (4)$$

$$\int \Re(\nu' - \nu, T, P) d\nu' = 1 \quad (5)$$

Which are, respectively, the aerosol attenuation factor due to iodine filter at the receiving frequency $\nu = \nu_0$, the attenuation factor for Cabannes-Brillouin scattering by the iodine filter, and the expression showing that the normalized Cabannes-Brillouin scattering function, $\Re(\nu, T, P)$ is used here. $F(\nu)$ is the transmission function of the iodine filter for the return signal. In Eq.1 and Eq.2, K_R and K_M are system constants, respectively, for reference and measurement channel, depending on total laser emission energy, optical efficiency and range factor; and Δr is the range resolution. β_a and β_m (α_a and α_m) are aerosol and molecular volume backscatter (extinction) coefficients, respectively.

Setting $f_a = 0$ in Eq.2, the atmospheric aerosol scattering ratio R_b can be expressed as:

$$R_b(r) = \frac{\beta_a(r)}{\beta_m(r)} = (1 + R_{bm}) \exp[D(r) - D_m] - 1 \quad (6)$$

$$D(r) = \ln[N_R(r) r^2] - \ln[N_M(r) r^2] \quad (7)$$

Where $D_m = D(r_m)$, $R_{bm} = R_b(r_m)$, and r_m is the height where R_b is minimum.

Using this method, the aerosol scattering ratio R_b can be measured with higher accuracy because it was not influenced by the variation of Rayleigh scattering spectrum with the atmospheric temperature.

3. EXPERIMENTAL RESULTS AND COMPARISONS

The observation place is located at Ocean University of China near the Yellow Sea coast, about 500m off the seashore. We measured aerosol scattering ratio (R_b) using our HSRL successfully, and the weather conditions include fine, cloudy and foggy. We compared the HSRL results with the rawinsonde balloon data which we can get twice (8:00 and 20:00) every day from Qingdao Observatory near our lidar system.

3.1 The aerosol profiles in the marine atmospheric boundary layer

Fig.3(a) shows the aerosol scattering ratio (R_b) profile under cloudy condition observed at 1257 UTC, Oct 21, 2005, from which we can get the base and top height of the cirrus, 10km and 12km respectively, and the optical depth can be calculated from the return signals. The aerosol concentration decreased gradually from the ground to 1km. Fig.3(b) shows the aerosol scattering ratio (R_b) profile in foggy observed at 1536 UTC Nov 9, 2005. The increase of the backscattering fraction is caused by fog, so R_b is about 26 near the ground, larger than that in fine day(Fig.3(b)), while the Relative Humidity (RH) is about 92% (Fig.3(c)). at the same altitude.

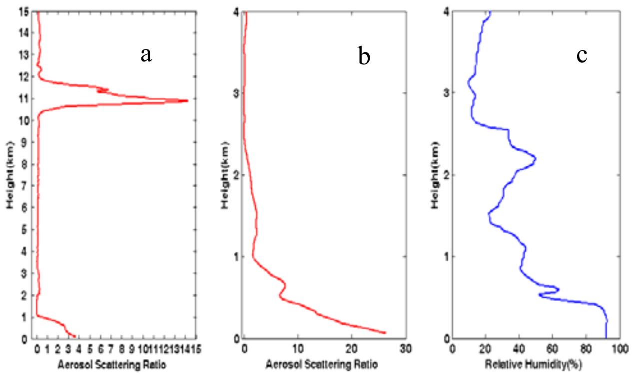

Fig. 3. (a) Aerosol scattering ratio, 1257 UTC, Oct 21, 2005
(b) Aerosol scattering ratio, 1536 UTC, Nov 9, 2005
(c) RH, 1200 UTC, Nov 9, 2005

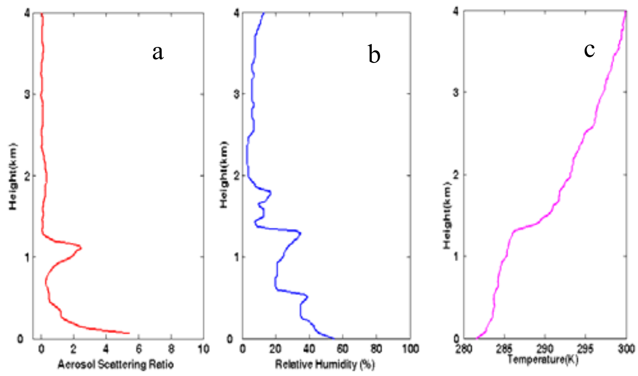

Fig. 4. (a) Aerosol scattering ratio, 1554 UTC, Apr 14, 2005,
(b) RH, 1200 UTC, Apr 14, 2005
(c) Potential temperature, 1200 UTC, Apr 14, 2005

From the Fig.4(a), we can see that there was an aerosol layer at height of about 1km. The main reason was the water vapor effect(Fig.4(b)), as well as a large potential temperature gradient (Fig.4(c)) .The profiles of aerosol and RH indicated multilayer character of MABL.

3.2 The profiles of aerosol and RH

Aerosol particles are known to absorb or release water in response to the changing RH of the atmosphere. As particles absorb or release liquid water, their physical and chemical properties such as size and index of refraction will change. Here, we have analyzed the correlation index between the profile of aerosol scattering ratio (R_b) and the RH. Fig.5 shows R_b and RH in cloudy condition, which correlation index is 0.90. The R_b ranges from 0 to 7 while RH 0~ 50 below 4km and both of them have a large gradient at 2km. When fog occurred, R_b would be very large caused by water vapor, which can be 26 while RH is 92% near the ground (Fig.6, the correlation index is 0.87). Under smoke condition, the main component of aerosol was not water vapor but dusts, so the index would be small（Fig.7, the correlation index is 0.70）. Fig.8 is the MODIS satellite image 1000 UTC, Nov 24, 2005. The weather is smoky known from Qingdao meteorological bureau.

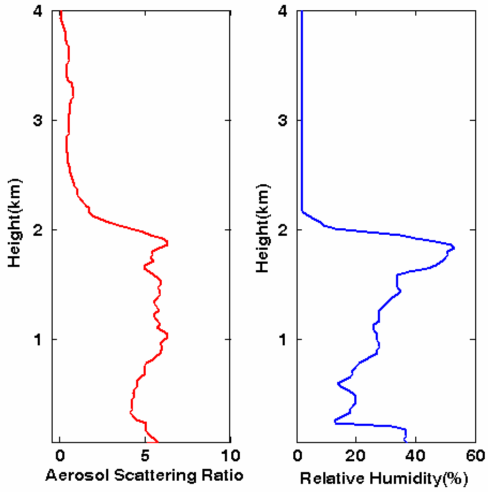

Fig.5. The correlation index is 0.90 between R_b(1315 UTC, Oct 16,2004)and RH(1200 UTC, Oct 16,2004)

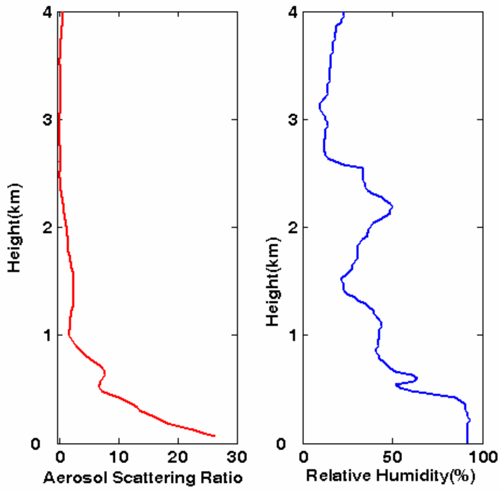

Fig.6. The correlation index is 0.87 between R_b(1536 UTC, Nov 9, 2005)and RH(1200 UTC, Nov 9, 2005)

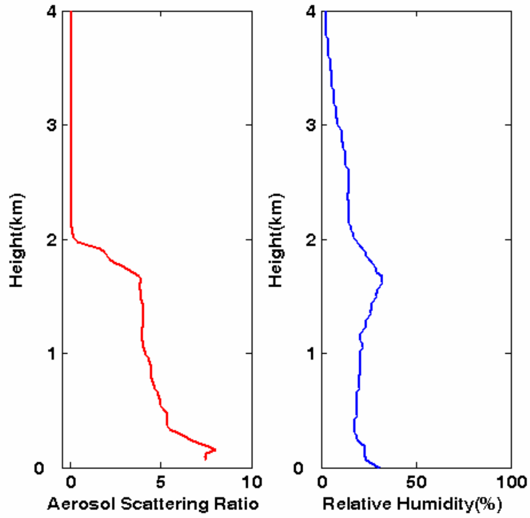

Fig.7. The correlation index is 0.70 between R_b(1321 UTC, Nov 24,2005)and RH(1200 UTC, Nov24,2005)

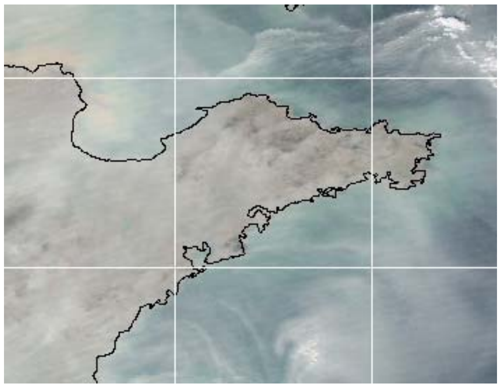

Fig.8. MODIS satellite, 10:00 UTC, Nov 24,2005, smoky

3.3 The height of the marine boundary layer

The height of the atmospheric boundary layer is one of the fundamental parameters that was used to characterize its structure (Gryning *et al*., 1987). The top of the MABL is generally marked by a temperature inversion as well as a large RH gradient. A wavelet method based on a Haar function (Davis *et al*., 2000) is used for analyzing for the aerosol scattering ratio profiles, then the marine boundary layer height is extracted from the profiles. The results were compared with the heights deduced from the profiles of potential temperature and RH(Fig.9-Fig.11). The results are summarized in Table 1.

4. CONCLUSION

In this observations, we can get some characters of the marine atmospheric boundary layer structure: (1)the correlation index between the aerosol scattering ratio(R_b) and RH is above 0.8 when fine and foggy, and the

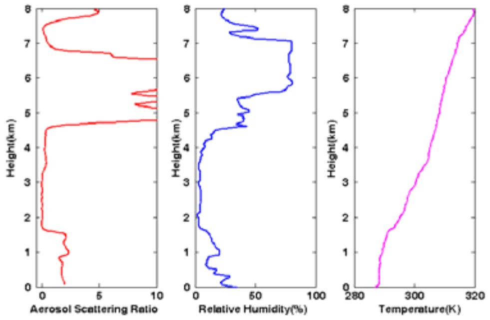

Fig.9. R_b (1331 UTC Nov 08, 2005), RH and potential temperature (1200 UTC Nov 08, 2005)

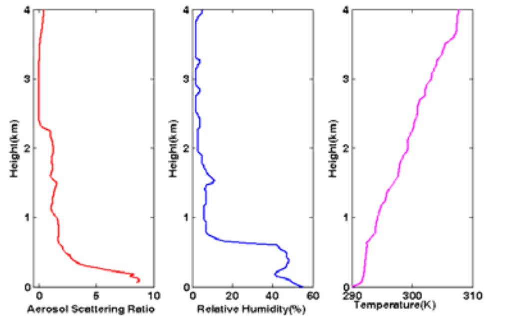

Fig.10. R_b(1321 UTC Nov 28, 2005), RH and potential temperature (1200 UTC Nov 28, 2005)

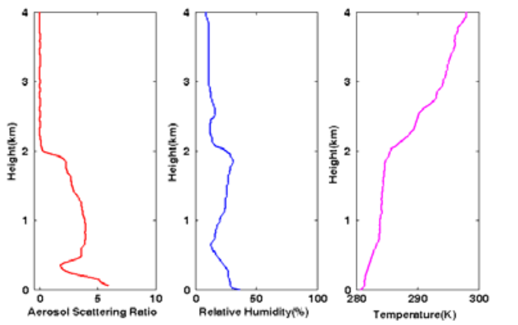

Fig.11. R_b(1338 UTC Nov 29, 2005), RH and potential temp (1200 UTC Nov 29 2005)

Date	R_b(km)	RH (km)	Potential temp (km)
08-11-2005	1.71	1.77	1.68
28-11-2005	1.68	1.62	1.32
29-11-2005	2.19	2.22	1.92

Table 1: MABL from the R_b of HSRL, RH and potential temperature from pilot balloon

correlation index is about 0.7 when smoky;(2) the top height of marine atmospheric boundary layer of the Yellow Sea near Qingdao is about 1.5km to 2.5km; (3) the multilayer phenomenon appeared sometimes.

5. ACKNOWLEDGEMENTS

This work was supported in part by National Natural Science Foundation of China (NSFC) project No. 40427001, No. 40275009 and No. 60578038.

6. REFERENCES

1. K. F. Fischer, V. J. Abreu, W. R. Skinner, J. E. Barnes, M. J. McGill, and T. D. Irgang, Visible wavelength Doppler lidar for measurement of wind and aerosol profiles during day and night, Opt. Eng. 34, 499–511,1995.

2. Z.S. Liu, D. Wu, J.T. Liu *et al.*, Low-Altitude atmospheric wind measurement from the combined Mie and Rayleigh backscattering by Doppler lidar with iodine filter,20 November 2002, vol.41, No.33, Applied Optics P7079-7086.

3. Z.S. Liu, W.B. Chen, T.L. Zhang, et al., An incoherent Doppler lidar for ground-based atmospheric wind profiling, Appl. Phys. B64, 561-566(1997).

4. G. Kaloshin, J. Piazzola *et al.*, Aerosol extinction spectral profiles in the marine atmospheric surface layer, Geophysical Research Abstracts, Vol.7, 00774, 2005

5. D. Katoshevski, A. Nenes *et al* , A study of processes that govern the maintenance of aerosols in the marine boundary layer, J. Aerosol Sci. Vol. 30, No.4, pp. 503-532,1999.

6. Chunlei Liu, Humidity effect on the aerosol particle spectra in the atmospheric boundary layer, J. Aerosol sci.,Vol.26,No.3, pp489-495,1995

7. M. Pahlow, J.Kleissl *et al.*, Atmospheric boundary-layer structure observed durng a haze event due to forest-fire smoke, Boundary-layer Meteorology(2005) 114:53-70.

8. James D. Klett, Lidar inversion with variable backscatter/extinction ratios, Applied Optics, Vol.24, No.11,1 June 1985.

9. E.Terradellas, G. Morales, Wavelet methods: application to the study of the stable atmospheric boundary layer under non-stationary conditions, Dynamics of Atmospheres and Oceans 34(2001) 225-244.

10. K.A. Edwards, A.M.Rogerson *et al.*, Adjustment of Marine Atmospheric Boundary layer to a Coastal Cape, American Meterological society, 15 June 2005.